Accepted Manuscript

Intersegmental Kinetics Significantly Impact Mapping from Finger Musculotendon Forces to Fingertip Forces

Dan Qiu, Sang Wook Lee, Mukarram Amine, Derek G. Kamper

PII: S0021-9290(17)30518-3
DOI: https://doi.org/10.1016/j.jbiomech.2017.10.004
Reference: BM 8404

To appear in: *Journal of Biomechanics*

Accepted Date: 1 October 2017

Intersegmental Kinetics Significantly Impact Mapping from Finger Musculotendon Forces to Fingertip Forces

Dan Qiu[1]*, Sang Wook Lee[2,3], Mukarram Amine[1] and Derek G. Kamper[4]

[1]Department of Biomedical Engineering, Illinois Institute of Technology, Chicago, IL; [2]Department of Biomedical Engineering, Catholic University of America, Washington, DC; [3]Center for Applied Biomechanics and Rehabilitation Research, MedStar National Rehabilitation Hospital, Washington, DC; [4]UNC/NC State Joint Department of Biomedical Engineering and Rehabilitation Engineering Core, North Carolina State University, Raleigh, NC/ University of North Carolina, Chapel Hill, NC

* Corresponding author

Dan Qiu, Ph.D.

Address: 3255 S Dearborn St, Chicago, IL 60616

Email: dqiu1@hawk.iit.edu

Telephone: +1-312-567-5100

Author Statement:

All authors were fully involved in the study and preparation of the manuscript. The material within this manuscript has not been and will not be submitted for publication elsewhere. There is no conflict of interest in the submission of this manuscript.

Word count: 3,442 (Introduction/Methods/Results/Discussion)

Abstract

Predicting the fingertip force vector resulting from excitation of a given muscle remains a challenging but essential task in finger biomechanical modeling. While the conversion of musculotendon force to fingertip force can significantly be affected by finger posture, current techniques utilizing geometric moment arms may not capture such complex postural effects. Here, we attempted to elucidate the postural effects on the mapping between musculotendon force and fingertip force through in vitro experiments. Computer-controlled tendon loading was implemented on the 7 index finger musculotendons of 5 fresh-frozen cadaveric hands across different postures. The resulting fingertip forces/moments were used to compute the effective static moment arm (ESMA), relating tendon force to joint torque, at each joint. The ESMAs were subsequently modeled in three different manners: independent of joint angle; dependent only upon the corresponding joint angle; or dependent upon all joint angles. We found that, for the reconstruction of the fingertip force vector, the multi-joint ESMA model yielded the best outcome, both in terms of direction and magnitude of the vector (mean reconstruction error < 4º in direction and < 2% in the magnitude), which indicates that intersegmental force transmission through a joint is affected by the posture of neighboring joints. Interestingly, the ESMA model that considers geometric changes of individual joints, the standard model used in biomechanical stimulations, often yielded worse reconstruction results than the simple constant-value ESMA model. Our results emphasize the importance of accurate description of the multi-joint dependency of the conversion of tendon force to joint moment for proper prediction of fingertip force direction.

Keywords

Index finger; Finger posture; Musculotendon; Fingertip force; Moment arm; Extensor mechanism; Force distribution

Introduction

In the fingers, musculotendon forces ultimately produce fingertip force/motion. As with other parts of the body, this mapping between the proximal musculotendon units and the distal fingertip is typically modelled using joint torques and forward dynamics or kinetics (Valero-Cuevas et al., 2009). Joint torques are estimated from tendon forces and moment arms, defined by the distance from joint center to the tendon. This technique is highly dependent upon accurate estimation of moment arm values, approximated in the past using methods such as anatomical geometry (Landsmeer, 1961), magnetic resonance imaging (Fowler et al., 2001), or tendon excursion (An et al., 1983; Franko et al., 2011).

The translation from muscle force to fingertip force or displacement, however, is especially complex. Most of the finger tendons cross multiple joints. On the palmar side of the finger, flexor tendons interact with annular and cruciate pulleys, potentially dissipating force or producing deformation of not only local but also adjacent pulley structures (Lin et al., 1990). On the dorsal side, several tendons merge into the extensor mechanism, an aponeurosis with multiple attachments to the underlying phalanges through various soft tissues (Garcia-Elias et al., 1991; Valero-Cuevas et al., 1998; Qian et al., 2014). These interactions between tendons and surrounding tissues could alter the mapping between tendon force and fingertip response, and their impact could be amplified by mechanical changes produced by kinematic and/or kinetic factors. Indeed, finger posture (Lee et al., 2008a and 2008b; Deshpande et al., 2010) and tendon loading conditions (Valero-Cuevas et al., 2007) have been shown to affect the force distribution within the extensor mechanism. The extent to which these factors impact the translation of musculotendon force to the force vector created at the fingertip, however, remains unclear.

Therefore, in this study, we examined the impact of loading level and multi-joint posture on the mapping of tendon to fingertip force. In accordance with the techniques employed in previous studies (Li et al., 2000; Valero-Cuevas et al., 2000; Lee et al., 2008a), we measured fingertip forces/moments resulting from different loads applied to individual musculotendon units in cadaveric specimens across different postures. From these forces, we computed effective static moment arm (ESMA) values, which describe the moment-generating capacity of a tendon from kinetic data (Lee et al., 2008b). We then created three different models of ESMA, each incorporating different degrees of postural influence: 1) no joint angle dependence, 2) dependence only on the corresponding joint angle, 3) dependence on multiple joint angles. We then used each model to predict the fingertip forces from the specific tendon loading. We hypothesized that the ESMA model considering the impact of multiple joints angles, not only the local joint as is typically done, would yield the most accurate prediction of the fingertip force.

Methods

Experimental Protocol

Five fresh-frozen hand specimens were obtained from 3 female donors, aged 72-87 years (mean: 79 years), with no known joint abnormalities. Each specimen was truncated at the mid-forearm and dissected to expose the tendons of the index finger. Using a WristJack, (Hand Biomechanics Laboratory, CA, USA), we fixed the wrist in a neutral position (Valero-Cuevas et al, 2000). Fingertip forces/moments were measured with a 6 degree-of-freedom (DOF) load cell (JR3 Inc., CA, USA) secured to the distal finger segment with screws (Fig. 1) (Lee et al., 2008a, 2008b). The average length (SD) of the proximal, middle and distal finger segments of the index fingers used in this study were 45.5(2.4), 22.8(1.5), and 22.6(2.0) mm, respectively.

The extrinsic tendons - flexor digitorum profundus (FDP), flexor digitorum superficialis (FDS), extensor digitorum communis (EDC), and extensor indicis (EI) - were each exposed proximal to the wrist and tied to a cable made of low-friction 0.4-mm diameter steel wire (BeadSmith, Helby Import Co., NJ, USA). For the intrinsic muscles - first dorsal interosseous (FDI), first palmar interosseous (FPI) and lumbrical (LUM) - a steel cable was tied around the tendon and then routed to follow the anatomical line of action of the muscle. The cable connected to LUM ran through the carpal tunnel, the FDI cable ran along the lateral side of the wrist, and the FPI cable ran along the back of the wrist. All of the cables subsequently passed through a panel to redirect them (Valero-Cuevas et al., 2000) toward a custom tendon actuation system (Fig. 2). Desired levels of tendon tension were applied by a servo-controlled tendon actuation system, based on a previous design (Huh and Lundberg, 2006). Stepper motors (43000 series, Haydon Kerk Inc., USA), controlled by a custom MATLAB (MathWorks, Waltham, MA) program, created the desired cable tension, as measured with linear force transducers (SB0-50, Transducer Techniques, CA, USA). The resulting fingertip forces and moments were recorded by the 6-DOF load cell at 200 Hz.

[Insert Figs. 1 and 2 about here]

All 7 index finger muscles were loaded individually at three different levels of force. Six muscles (FDP, FDS, EDC, EI, FPI and LUM) were loaded at 5%, 10% and 15% of their maximum isometric force and FDI was tested at lower values of 2.5%, 5% and 7.5% of maximum force. Forces of 15% or less were used to avoid producing finger joint angle changes, which may arise due to joint laxity. The maximum force of each tendon was estimated using muscle cross-sectional areas measured from *in vivo* ultrasound images of ten healthy subjects (Triandafilou and Kamper, 2012) and a specific tension of 35 N/cm^2 (Zajac, 1989).

We tested each load at 12 different postures across the joint range of motion, encompassing all combinations of the elements of the set of metacarpophalangeal (MCP) joints {0°, 30°, 60°} with the elements of the set of the proximal and distal interphalangeal (PIP, DIP) joints {(0°,0°), (30°,0°), (45°,15°), (60°,30°)}. PIP and DIP angles were varied together as physiological constraints limit independent movements. Specimens were sprayed with a saline solution every 5 minute to prevent desiccation.

Data Analysis

Fingertip force: For each trial, we calculated the fingertip force/moment vector as the mean value across a one-second data window positioned at least 5 seconds after the tendon load reached the desired steady-state value. Each fingertip force vector was projected onto the sagittal plane, and the magnitude and the angle were computed. To characterize fingertip forces across the specimens, the mean and standard deviation of both the magnitude and direction of the measured fingertip force vectors were calculated, as performed in previous studies for the thumb (Towles et al., 2008; Wohlman and Murray, 2013).

ESMA estimation: From these data, we computed the ESMAs of each muscle at each joint (Kamper et al., 2006; Lee et al., 2008b) for each specimen. Measured fingertip forces and moments resulting from tendon loading were transformed into joint torques using the Jacobian (Valero-Cuevas et al., 1998; Kamper et al., 2006). ESMA was then computed from the ratio of the joint torque to the known tendon load. Note that, because of potential force dissipation and distribution, ESMA may differ from kinematic moment arm values (An et al., 1979; An et al., 1983). An analysis of variance (ANOVA) was performed on the dependent variables of ESMA, with the independent variables of tendon load, IP posture, and MCP posture.

Effect of tendon load: To examine the impact of level of musculotendon force directly on the fingertip force, we performed linear regression between the applied tendon force magnitude and resulting three fingertip force components (palmar, lateral, distal). R^2-values were computed, then p-values were examined for goodness of fit.

ESMA modeling: Potential postural effects on ESMA values were modeled using the following three regression models, each of which was consequently used to predict/reconstruct the fingertip force vector.

For model 1, the average ESMA of given joint across specimens and postures was simply used as the moment arm (a_0^i: i = 1: DIP; 2: PIP; 3: MCP). The value remained fixed and did not change with joint angle (Eq. 1).

$$R_i = a_0^i \tag{1}$$

For model 2, ESMA was modeled as a function of solely the corresponding joint angle, in accordance with classical estimation based on geometric considerations (Landsmeer, 1961; Biggs and Horch, 1999). Here, ESMA data for each joint were fit to a 2nd-order polynomial of the corresponding joint; the 2nd-order term was used to explain possible nonlinearity in the relationship between finger joint rotation and its moment arm (Deshpande et al., 2010; Kociolek and Keir, 2016), using multiple regression (Eq. 2).

$$R_i = b_0^i + b_1^i \theta_i + b_2^i \theta_i^2 \tag{2}$$

where θ_1 : DIP, θ_2 : PIP, θ_3 : MCP joint flexion angles.

For model 3, moment arms were computed using regression analysis to fit a 2nd-order polynomial involving all three joint angles (Eq. 3). Here, PIP and DIP joint angles were summed to create the angle θ_{IP}, and the moment arm values were modeled as a 2nd-order polynomial of both θ_{IP} and θ_{MCP}, accounting for the effect of joint posture on the force transmission from adjacent segments. Additionally, in order to capture possible interactions between MCP and IP angles, an interaction term was included in this MCP model:

$$\mathrm{R_i} = \mathrm{c_0^i} + \mathrm{c_1^i}\theta_{\mathrm{IP}} + \mathrm{c_2^i}\theta_{\mathrm{IP}}^2 + \mathrm{c_3^i}\theta_{\mathrm{MCP}} + \mathrm{c_4^i}\theta_{\mathrm{MCP}}^2 + \mathrm{c_5^i}\theta_{\mathrm{IP}}\theta_{\mathrm{MCP}} \tag{3}$$

where $\theta_{\mathrm{IP}} = \theta_1 + \theta_2$ and $\theta_{\mathrm{MCP}} = \theta_3$.

The model 3 attempts to account for the effects of intersegmental kinetics on the joint moment by modeling ESMA values (converting tendon force to joint moment) as functions of all joint angles. For the tendons within the extensor mechanism, rotation of distal joints (DIP/PIP) could result in localized strain of the extensor mechanism (Lee et al., 2008a), which in turn affects the tendon force distribution to the tendon slips, as shown in our simulation study (Lee and Kamper, 2016). For the long flexor tendons, each pulley deforms as the adjacent joint rotates, which could also affect overall tendon geometry (Zhao et al., 2000; Tang and Xie, 2001).

Fingertip force reconstruction: For each specimen, fingertip force vectors at the highest force level tested (15% of maximal force except FDI; 7.5% for FDI) were computed/reconstructed using the ESMA values estimated by each of the three different models across all conditions except one. The IP posture of (PIP, DIP) = (0º, 0º) was excluded from this analysis due to the singularity produced in the Jacobian matrix. Thus, a total of 63 force vectors were computed (7 musculotendons × 3 MCP postures × 3 IP postures).

The reconstructed force vectors were compared to the fingertip force vector recorded during the cadaveric experiments, and the following error values were estimated (Eq. 4): absolute/relative error in the force magnitude (ε_M and $\hat{\varepsilon}_M$), and absolute error in the force direction (ε_α).

$$\begin{aligned} \varepsilon_M &= \|\hat{\mathbf{f}} - \mathbf{f}\| \\ \hat{\varepsilon}_M &= \|\hat{\mathbf{f}} - \mathbf{f}\| / \|\mathbf{f}\| \\ \varepsilon_\alpha &= \cos^{-1}\left[\hat{\mathbf{f}} \cdot \mathbf{f} / \left(\|\hat{\mathbf{f}}\|\|\mathbf{f}\|\right)\right] \end{aligned} \tag{4}$$

Here, $\mathbf{f}$ denotes the fingertip force vector obtained during cadaveric experiment, and $\hat{\mathbf{f}}$ the reconstructed fingertip force vector.

Results

Testing was completed for all muscles on all 5 specimens with the exception of EI for one specimen (right hand); the EI muscle was absent in this specimen although this muscle was present and appeared normal in the donor's other (left) hand. Lack of EI in some specimens has been reported in the literature (Mestdagh et al., 1985). Additionally, experimental data from the loading of the FDI muscle for one specimen were excluded due to abnormal fingertip force direction, which deviated by more than 90° from the results of other specimens. This aberration may have resulted from undetected damage of the tendon or constraining ligaments.

ESMA modeling

Experimentally derived ESMA: The fingertip force increased with tendon force in a highly linear manner. Across all seven muscles and all fingertip force directions (palmar, lateral, and distal), the mean (SD) R^2 value for the regression fit between the two forces was 0.963 (0.018). R^2 was highest for LUM (mean $R^2 = 0.992$) and FDS (mean $R^2 = 0.972$), and lowest for EI (mean $R^2 = 0.948$) and EDC (mean $R^2 = 0.933$). Significant goodness of fit was apparent for all 7 muscles ($p < 0.001$). There was also no significant effect of tendon load level on the joint moments (computed from fingertip forces through Jacobian), and thus no significant effect on the ESMA values.

ESMA values of all three joints for all 7 musculotendons were, however, significantly affected by the IP posture (all p-values < 0.001). MCP posture affected only the MCP ESMA values of the extrinsic flexor tendons (FDP, FDS: $p < 0.001$) and FPI ($p = 0.002$) (Table 1). When MCP joint flexion increased from 0° to 60°, the MCP ESMA mean ± SD values for FDP and FDS increased from 16.8 ± 0.2mm to 19.7 ± 0.2mm and from 21.3 ± 0.2mm to 23.4 ± 0.1mm, respectively. Conversely, for FPI, MCP ESMA decreased from 4.40 ± 4.28mm to 1.40 ± 7.77mm when MCP flexion increased from 0º to 60º.

Interactions between MCP and IP postures were found to significantly affect ESMAs in those musculotendons with significant MCP effects (i.e., FPI, FDP and FDS). For all three of these tendons, MCP angle had the greatest impact on MCP ESMA when the IP joints were extended, i.e., IP = (0°, 0°).

[Insert Table 1 about here]

ESMA values computed from posture models: Among the three models, Model 3 (all joint angles) resulted in the lowest error in the ESMA values while Model 1 (no joint angle dependence) generated the highest error values (Table 2). Notably, for Model 2, the mean error in the MCP ESMA value was much greater than that computed for the other joints (3-fold increase from DIP ESMA error; 2-fold increase from PIP ESMA error; Table 2). This indicates a substantial IP-posture dependence (see Figs. 3 and 4).

[Insert Table 2 and Figs. 3 and 4 about here]

Fingertip force prediction/reconstruction

Differences in ESMA values across models led to substantial variances in fingertip force prediction in some cases. Out of the three models, model 3, which accounts for the effects of intersegmental kinetics on force-moment conversion, yielded the most accurate reconstruction of the fingertip force vectors for all 7 musculotendons (Table 3). Across all muscles, magnitude error was less than 2% and angle error less than 4°.

[Insert Table 3 about here]

Interestingly, the model for which ESMA was a function of the corresponding joint only (model 2) resulted in the worst reconstruction results, especially for the extrinsic muscles (Fig. 5). Error in fingertip force direction exceeded 12° and magnitude error exceeded 5% for FDP. For the extrinsic extensors, direction of the predicted fingertip force differed from the actual direction by over 20° for EDC and over 17° for EI.

[Insert Fig. 5 about here]

Discussion

Effects of posture on force-to-moment conversion (ESMA)

Consistent with previous studies, including kinematic studies, we found that finger posture significantly impacted ESMA values (An et al., 1983; Kamper et al., 2006; Lee et al., 2008b). However, we found that IP posture not only affected the ESMA at the DIP and PIP joints, but also significantly impacted the ESMA at the MCP joint for all muscles. Inclusion of all three finger joint angles resulted in the best fit to the experimentally determined values. This effect is not accounted for in methods such as the tendon excursion, which look at joints traversed by multiarticular tendons in isolation. In contrast, our novel modeling method, which computes ESMA values from all joint angles (both IP and MCP), was able to capture such multi-joint dependency of the tendon force-to-joint moment conversion.

Several mechanisms may contribute to the multiarticular effects of posture on force-to-moment conversion (i.e., ESMA). For the extensor musculotendons, the IP flexion could significantly change the geometry of the extensor mechanism, thereby affecting configuration of the inter-tendon connection (Garcia-Elias et al., 1991) and/or connection to the surrounding ligaments (Harris and Rutledge, 1972). A previous *in vitro* study (Valero-Cuevas et al., 2007) also found that the local geometry of the tendon network may significantly affect distribution of the tendon force (although that study examined changes produced by altering tendon force condition, not by changing posture). The extensor mechanism does not insert into the proximal phalanx, which may explain lack of an impact of MCP joint angle on the ESMA values of most of the musculotendons connecting to the extensor mechanism (EDC, EI, LUM, and FDI). For the flexor tendons, the tendon path is constrained by annular and cruciform pulleys (Doyle, 1988). Not only does each pulley deform as the adjacent joint rotates (Schweizer, 2001), but such deformation could also affect the moment arm of neighboring pulleys (Zhao et al., 2000; Tang and Xie, 2001).

Here, it should be acknowledged that the proposed method (ESMA) cannot differentiate the impact of these different mechanisms (e.g., force dissipation to surrounding tissues, frictional loss inside pulleys, etc.) on the tendon force-joint moment conversion, since the ESMA values are lumped parameters that experimentally quantify the effects of these various mechanisms on the fingertip force measurements. Further experiments involving local stress/strain measurements would be required to precisely gauge the contribution of these different force dissipation mechanisms to the overall force transformation efficiency.

Lack of effect of tendon load on ESMA

In contrast, the magnitude of the tendon load did not have a significant impact on the computed ESMA, as the relationship between tendon force and fingertip force was found to be linear. Thus, ESMA remained constant across loading levels and was independent of load. It should be noted that musculotendons were loaded to only 15% (7.5% for FDI) of maximum voluntary forces, so the possibility exists that this linearity is not maintained at higher loads, although the linear relationship has been reported for greater loading levels (Valero-Cuevas et al., 2000; Lee et al., 2008). Additionally, as we examined loading of a single tendon, it is not clear whether simultaneous loading of multiple tendons would exhibit the same linearity, although previous research has suggested that it would (Valero-Cuevas et al., 2000).

Importance of modeling posture dependence in reconstructing fingertip force

As the relationship between ESMA and fingertip force is non-linear, errors in predicting ESMA can lead to even greater errors in fingertip force. Among the different models, Model 3, including a dependence of ESMA upon angles of all joints, produced the best reconstruction of the fingertip force vector, thus supporting our hypothesis. This model was based upon the assumption that the intersegmental force transmission via the mechanisms explained above plays an important role in the transformation of individual musculotendon force to fingertip force. Importantly, use of the standard moment arm model (Model 2) which includes a dependence only upon the angle of the corresponding joint, yielded the worst prediction of fingertip force. Errors were greater than when no joint dependence at all was included.

Interestingly, despite the lack of statistical significance of the effect of MCP angle on ESMA, disregarding the influence of MCP joint angle on ESMA also degraded reconstruction accuracy.. We ran a *post hoc* analysis which entailed removing the MCP terms from Model 3. Without the MCP terms, prediction of fingertip force worsened, most likely due to the sensitivity of the Jacobian to MCP joint posture. Small errors in MCP torque could produce relatively large errors in fingertip force.

Implications/Methodological consideration

Our results of fingertip force reconstruction show that it is critical to consider multi-joint dependency in the kinetic conversion of tendon force to joint moment when using the latter to reconstruct the fingertip force vector. In particular, changes in the IP joint posture significantly affected the MCP ESMA values, indicating that intersegmental force transmission through the MCP joint was affected by the posture of neighboring joints (DIP, PIP). Such multi-joint dependency was found critical in reconstructing the fingertip force vector based on tendon force information.

Some limitations of this study should be acknowledged. The magnitudes of obtained ESMA values appear to be smaller than the moment arm values measured in other studies. This may have resulted from all of our specimens coming from a relatively small number of females. These limitations, however, do not necessarily affect the generalization of the mapping relationships obtained in this study to larger hands. While including more specimens of both genders would likely alter the absolute values of the mean and standard deviation for the ESMA, we expect the nature of the mapping from the tendon force to the fingertip force, such as described by Model 3, to remain the same. Inherently, the use of cadaver specimens raises the concern of changes in mechanical properties due to desiccation resulting from exposure to the air. To examine the impact of repeated exposures, two specimens were retested after having been exposed to the air on 5-6 separate occasions (far exceeding what was done for this study). Interestingly, while the long flexor tendons were not significantly affected (no substantial changes in resultant forces), some retest results for EDC/EI fingertip force direction differed from the original results by as much as 70°. The extensor mechanism thus seems to be especially susceptible to dehydration. We sprayed specimens frequently with saline and minimized total experiment time in order to mitigate these potential issues.

Conclusion

We elucidated the mapping between musculotendon force and fingertip force and its posture-dependency via cadaveric experiments. Transformation of the tendon force to the fingertip force was not affected by the force magnitude. However, conversion of the tendon force to the joint moment (ESMA) was significantly affected not only by the corresponding joint angle, but also by neighboring joint angles, which consequently affected the fingertip force estimation. Our results suggest that the intersegmental force transmission at each joint can be influenced by the posture of the neighboring joints, which should be carefully considered for proper fingertip force reconstruction.

Acknowledgements

The work was in part supported by National Science Foundation (CBET: 1452763) and the National Institutes of Health (NINDS: 1R01NS052369-01A1).

References:

An, K, N., Chao, E. Y., Cooney, W. P., Linscheid, R.L., 1979. Normative model of human hand for biomechanical analysis, Journal of Biomechanics 12, 775-788.

An, K. N., Ueba, Y., Chao, E. Y., Cooney, W. P., Linscheid, R. L., 1983. Tendon excursion and moment arm of index finger muscles, Journal of Biomechanics 16, 419-425.

Biggs, J., Horch, K., 1999. A three-dimensional kinematic model of the human long finger and the muscles that actuate it, Medical Engineering Physics 21, 625-639.

Deshpande, A. D., Balasubramanian, R., Ko, J., Matsuoka, Y., 2010. Acquiring variable moment arms for index finger using a robotic testbed, IEEE Transactions on Biomedical Engineering 57, 2034-2044.

Doyle, J. R., 1988. Anatomy of the finger flexor tendon sheath and pulley system, Journal of Hand Surgery 13A, 473-484.

Fowler, N. K., Nicol, A. C., Condon, B., Hadley, D., 2001. Method of determination of three dimensional index finger moment arms and tendon lines of action using high resolution MRI scans, Journal of Biomechanics 34, 791-797.

Franko, O. I., Winters, T. M., Tirrell, T. F., Hentzen, E. R., Lieber, R. L., 2011. Moment arms of the human digital flexors, Journal of Biomechanics 44, 1987-1990.

Garcia-Elias, M., An, K. N., Berglund, L., Linscheid, R. L., Cooney, W. P., Chao, E. Y., 1991. Extensor mechanism of the fingers. I. A quantitative geometric study, Journal of Hand Surgery 16A, 1130-1136.

Harris, C., Rutledge, G. L., 1972. The functional anatomy of the extensor mechanism of the finger, Journal of Bone and Joint Surgery 54A, 713-726.

Huh, H., Lundberg, F., 2006. Design of a mechatronic interface for simulating tendon transfer in cadaveric hands, KTH, Sweden. Master of Science.

Kamper, D. G., Fischer, H. C., Cruz, E. G., 2006. Impact of finger posture on mapping from muscle activation to joint torque, Clinical Biomechanics 21, 361-369.

Kociolek, A. M., Keir, P. J., 2015. Development of a kinematic model to predict finger flexor tendon and subsynovial connective tissue displacement in the carpal tunnel, Ergonomics 58, 1398-1409.

Landsmeer, J. M. F., 1961. Studies in the anatomy of articulation. I. The equilibrium of the intercalated bone. Acta Morphologica Neerlander_Scandinavica 3, 287–303

Lee, S. W., Chen, H., Towles, J. D., Kamper, D. G., 2008a. Effect of finger posture on the tendon force distribution within the finger extensor mechanism, Journal of Biomechanical Engineering 130, 051014.

Lee, S. W., Chen, H., Towles, J. D., Kamper, D. G., 2008b. Estimation of the effective static moment arms of the tendons in the index finger extensor mechanism, Journal of Biomechanics 41, 1567-1573.

Lee, S. W., Kamper, D. G., 2016. A novel computational modeling explains postural effects on strain distribution in finger extensor apparatus, Proceedings of the 40th Annual Conference of American Society of Biomechanics, Raleigh, NC.

Li, Z. M., Zatsiorsky, V. M., Latash, M. L., 2000. Contribution of the extrinsic and intrinsic hand muscles to the moments in finger joints, Clinical Biomechanics 15, 203-211.

Mestdagh, H., Bailleul, J. P., Vilette, B., Bocquet, F., Depreux, R., 1985. Organization of the extensor complex of the digits, Anatomia Clinica 7, 49-53.

Qian, K., Traylor, K., Lee, S. W., Ellis, B., Weiss, J. A., Kamper, D. G., 2014. Mechanical properties vary for different regions of the finger extensor apparatus, Journal of Biomechics 47, 3094-3099.

Schweizer, A., 2001. Biomechanical properties of the crimp grip position in rock climbers, Journal of Biomechanics 34, 217-223.

Tang, J. B., Xie, R. G., 2001. Effect of A3 pulley and adjacent sheath integrity on tendon excursion and bowstringing, Journal of Hand Surgery 26A, 855–861

Towles, J. D., Hentz, V. R., Murray, W. M., 2008. Use of intrinsic thumb muscles may help to improve lateral pinch function restored by tendon transfer, Clinical Biomechanics 23, 387-394.

Triandafilou K. M., Kamper D. G. 2012. Investigation of hand muscle atrophy in stroke survivors, Clinical Biomechanics 27, 268-272.

Valero-Cuevas, F. J., Zajac F. E., Burgar C. G., 1998. Large index-fingertip forces are produced by subject-independent patterns of muscle excitation, Journal of Biomechanics 31, 693-703.

Valero-Cuevas, F. J., Towles J. D., Hentz V. R., 2000. Quantification of fingertip force reduction in the forefinger following simulated paralysis of extensor and intrinsic muscles, Journal of Biomechanics 33, 1601-1609.

Valero-Cuevas, F. J., Yi, J. W., Brown, D., McNamara, R. V., Paul, C., Lipson, H., 2007. The tendon network of the fingers performs anatomical computation at a macroscopic scale, IEEE Transactions on Biomedical Engineering 54, 1161-1166.

Valero-Cuevas, F. J., Hoffmann, H., Kurse, M. U., Kutch, J. J., Theodorou, E. A., 2009. Computational models for neuromusulcar function, IEEE Reviews in Biomedical Engineering 2, 110-135.

Wohlman, S. J., Murray, W. M., 2013. Bridging the gap between cadaveric and *in vivo* experiments: a biomechanical model evaluating thumb-tip endpoint forces, Journal of Biomechanics 46, 1014-1020.

Zajac, F. E., 1989. Muscle and tendon: properties, models, scaling, and application to biomechanics and motor control, Critical Reviews in Biomedical Engineering 17, 359-411.

Zhao, C. F., Amadio, P. C., Berglund, L., An, K. N., 2000. The A3 pulley, Journal of Hand Surgery 25A, 270-276.

List of Tables

Table 1

Posture	ESMA	Tendon						
		EDC	EI	FDI	FPI	LUM	FDP	FDS
IP	Total	**< 0.001**	**< 0.001**	**< 0.001**	**< 0.001**	**< 0.001**	**< 0.001**	**< 0.001**
	DIP*	**< 0.001**	**< 0.001**	**< 0.001**	**< 0.001**	**< 0.001**	**< 0.001**	**< 0.001**
	PIP*	**< 0.001**	**0.002**	**< 0.001**	**< 0.001**	**< 0.001**	**< 0.001**	**< 0.001**
	MCP*	**< 0.001**	**0.001**	**< 0.001**	**< 0.001**	**< 0.001**	**< 0.001**	**< 0.001**
MCP	Total	0.660	0.292	0.550	**0.002**	0.095	**< 0.001**	**< 0.001**
	DIP*	0.906	0.828	0.266	0.863	0.455	0.059	0.172
	PIP*	0.775	0.411	0.218	0.393	0.396	**0.035**	**0.046**
	MCP*	0.889	0.275	0.143	**0.029**	0.218	**0.004**	**0.001**
IP×MCP	Total	0.788	0.282	0.944	**0.028**	0.441	**0.001**	**< 0.001**
	DIP*	0.502	0.298	0.382	**0.004**	0.657	0.065	**0.002**
	PIP*	0.592	0.424	0.227	**0.015**	0.537	0.131	**0.001**
	MCP*	0.652	0.281	0.215	**0.014**	0.358	0.165	**0.001**

* Bonferroni correction for multiple comparisons

Table 2

	DIP	PIP	MCP	Average
Model 1	1.46 (0.40)	1.93 (0.52)	1.77 (0.52)	1.72 (0.50)
Model 2	0.54 (0.25)	0.86 (0.34)	1.63 (0.54)	1.01 (0.60)
Model 3	0.25 (0.12)	0.38 (0.14)	0.40 (0.14)	0.34 (0.14)

Table 3

Tendon	Error	Model 1	Model 2	Model 3
EDC	ΔM (%)	2.49 (1.45)	5.38 (2.84)	0.69 (0.38)
	Δθ (º)	10.98 (7.11)	20.96 (14.75)	3.01 (1.76)
EI	ΔM (%)	1.83 (1.52)	4.30 (3.30)	0.64 (0.71)
	Δθ (º)	8.30 (6.85)	17.25 (19.10)	3.11 (3.34)
FDI	ΔM (%)	1.51 (1.27)	3.83 (2.22)	0.72 (0.23)
	Δθ (º)	2.75 (1.59)	2.97 (1.93)	1.50 (1.01)
FPI	ΔM (%)	4.00 (1.78)	3.93 (3.27)	0.90 (0.79)
	Δθ (º)	5.21 (4.33)	4.83 (3.83)	0.66 (0.41)
LUM	ΔM (%)	6.05 (4.08)	6.66 (6.65)	1.15 (0.84)
	Δθ (º)	2.87 (1.81)	1.14 (0.57)	0.53 (0.24)
FDP	ΔM (%)	5.89 (5.57)	5.50 (4.38)	1.03 (0.56)
	Δθ (º)	9.36 (11.77)	12.41 (11.40)	1.82 (2.09)
FDS	ΔM (%)	5.98 (4.20)	3.70 (2.75)	0.72 (0.34)
	Δθ (º)	8.16 (6.53)	6.59 (4.89)	1.14 (0.53)

List of Figures

Fig. 1. Anatomy of fingertip force production: (a) Tendons and other anatomical components of the finger musculotendon structure associated with fingertip force production; (b) Definition of six orthogonal fingertip force directions with respect to the distal phalanx.

Fig. 2. Experimental setup for the measurement of fingertip force/moment in cadaveric specimen. The specimen (on the left) was mounted on a WristJack fixation jig. The tendons were loaded by the automatic tendon actuation system (on the right), designed based on GRASP project of Stanford University (Huh and Lundberg 2006).

Fig. 3. EDC ESMA modeling using different models: (Column a) Model 1 (no joint dependence); (Column b) Model 2 (ESMA dependent on angle of corresponding joint); (Column c) Model 3 (ESMA dependent on angles of all joints). ESMA values shown for: top row - distal interphalangeal (DIP) joint; middle row – proximal interphalangeal (PIP) joint; bottom row - metacarpophalangeal (MCP) joint. ESMA value shown for each of the 9 IP and MCP postures for each model. Best fit is obtained with Model 3.

Fig. 4. FDP ESMA modeling using different models: (a) Model 1; (b) Model 2; (c) Model 3. ESMA values shown for: top row - distal interphalangeal (DIP) joint; middle row – proximal interphalangeal (PIP) joint; bottom row - metacarpophalangeal (MCP) joint. ESMA value shown for each of the 9 IP x MCP postures for each model. Best fit is obtained with Model 3.

Fig. 5. Comparison of the fingertip force vectors obtained from the experimental data (black) and reconstructed from the different ESMA models: Model 1(red), Model 2 (green), Model 3 (blue). (a) loading of EDC tendon; (b) loading of FPI musculotendon; (c) loading of FDP tendon. Model 3 provides the best fit, typically covering the black line representing the experimental data.

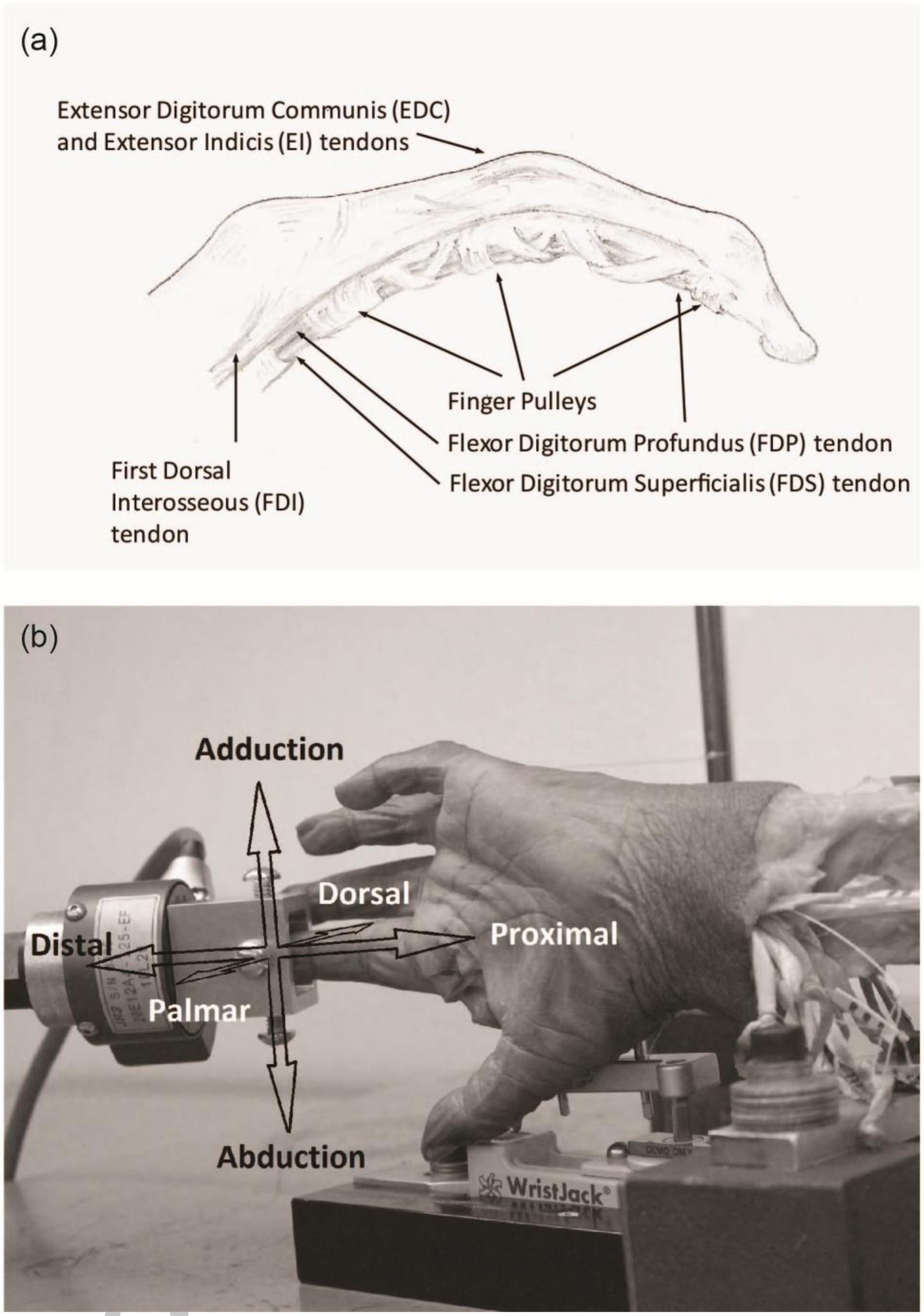
(a)
Extensor Digitorum Communis (EDC)
and Extensor Indicis (EI) tendons
Finger Pulleys
Flexor Digitorum Profundus (FDP) tendon
Flexor Digitorum Superficialis (FDS) tendon
First Dorsal
Interosseous (FDI)
tendon
(b)
Adduction
Dorsal
Distal
Proximal
Palmar
Abduction
WristJack®

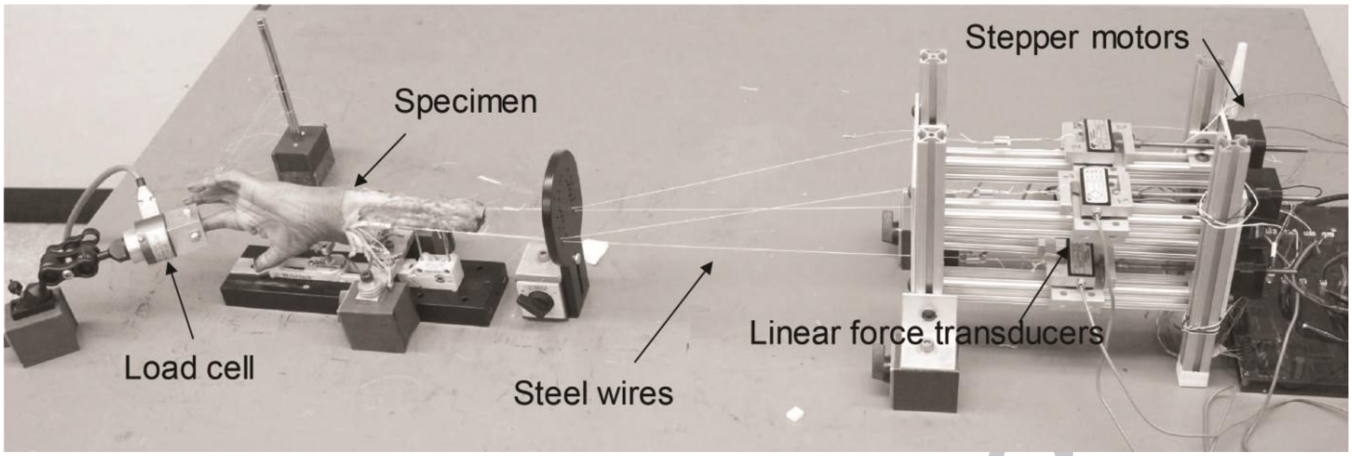
Stepper motors
Specimen
Load cell
Steel wires
Linear force transducers

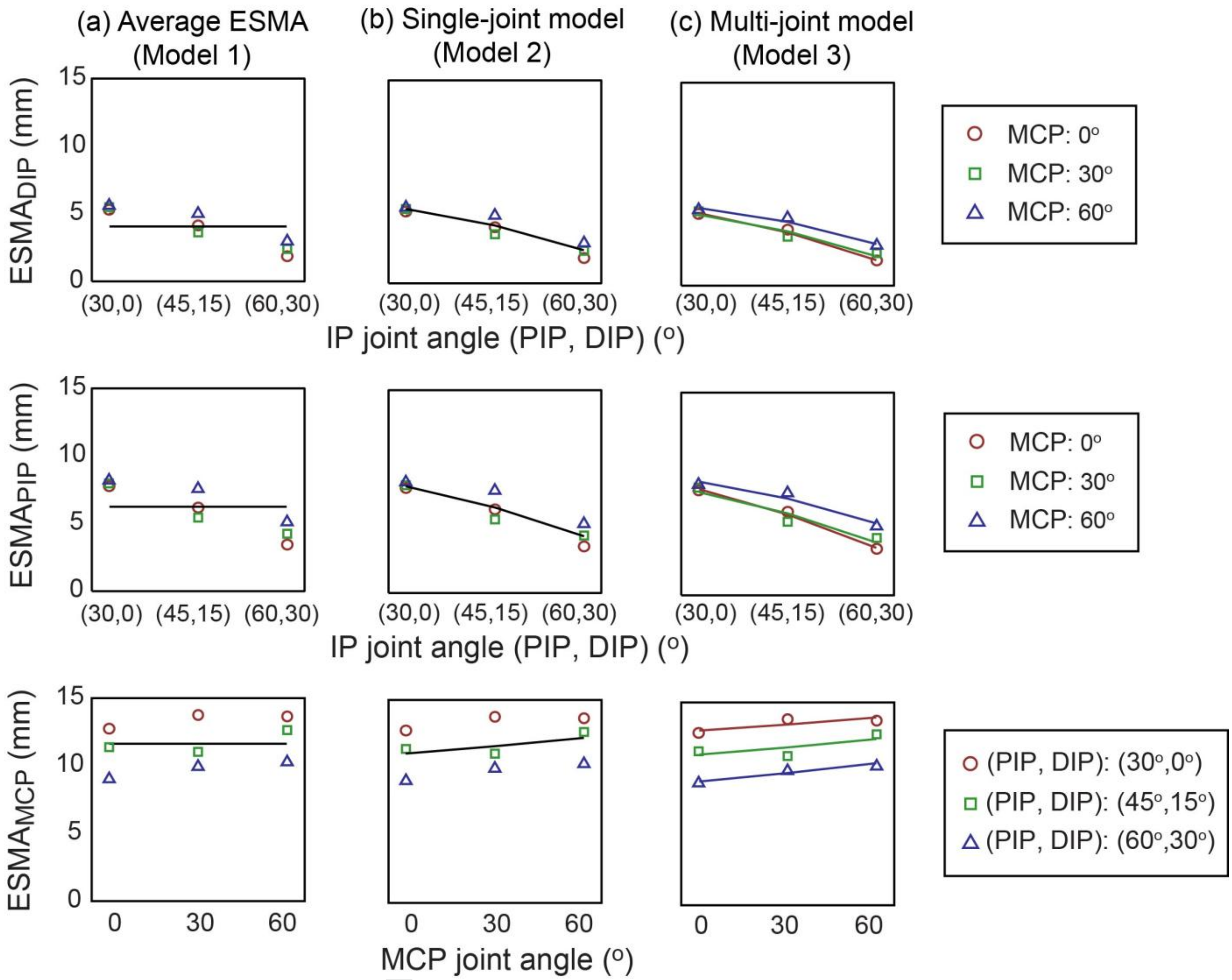
(a) Average ESMA (Model 1)
(b) Single-joint model (Model 2)
(c) Multi-joint model (Model 3)
ESMADIP (mm)
ESMAPIP (mm)
ESMAMCP (mm)
15
10
5
0
(30,0) (45,15) (60,30)
IP joint angle (PIP, DIP) (o)
0 30 60
MCP joint angle (o)
MCP: 0o
MCP: 30o
MCP: 60o
(PIP, DIP): (30o,0o)
(PIP, DIP): (45o,15o)
(PIP, DIP): (60o,30o)

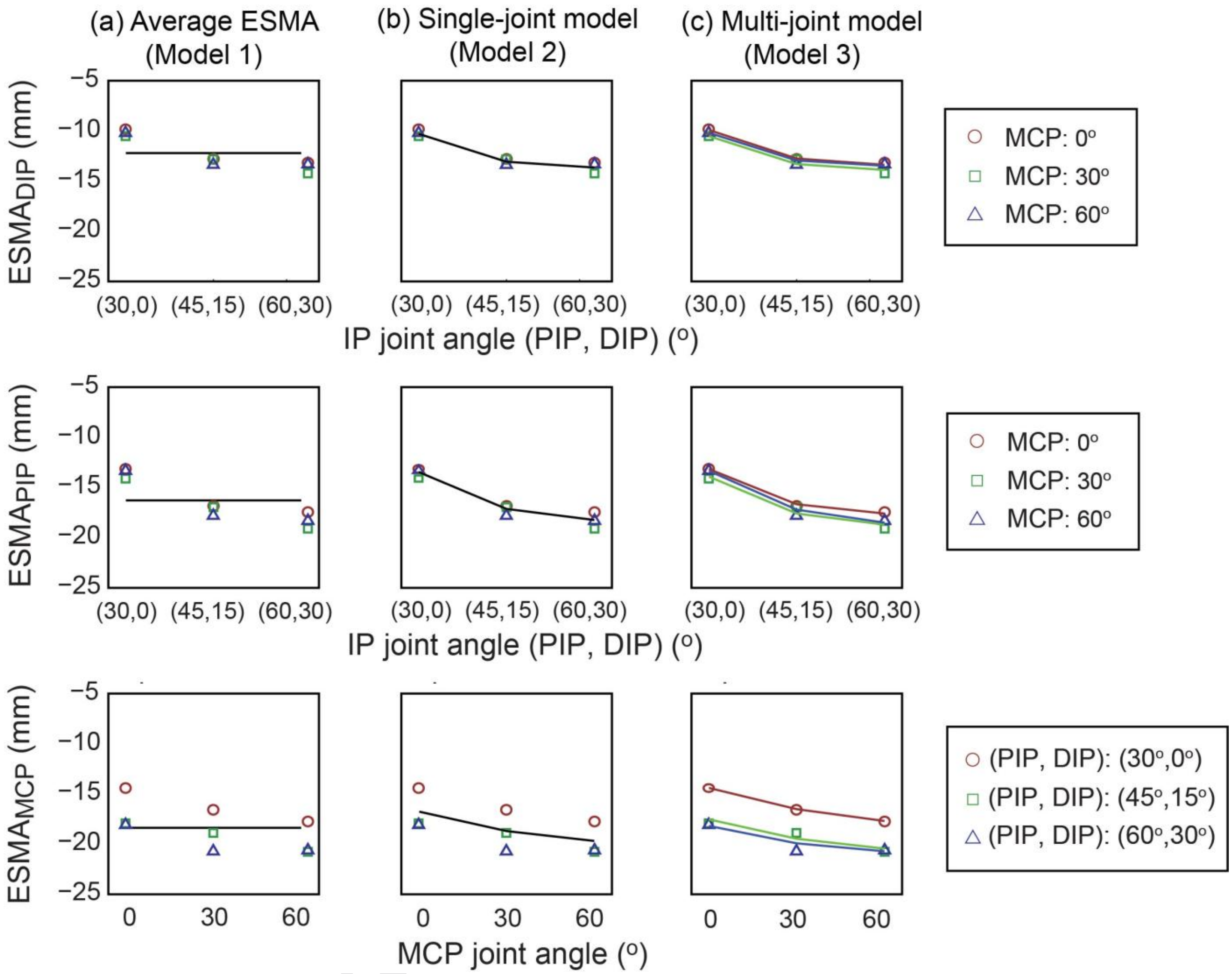

(a) Average ESMA (Model 1)
(b) Single-joint model (Model 2)
(c) Multi-joint model (Model 3)
ESMADIP (mm)
ESMAPIP (mm)
ESMAMCP (mm)
−5
−10
−15
−20
−25
(30,0) (45,15) (60,30)
IP joint angle (PIP, DIP) (o)
MCP: 0o
MCP: 30o
MCP: 60o
0 30 60
MCP joint angle (o)
(PIP, DIP): (30o,0o)
(PIP, DIP): (45o,15o)
(PIP, DIP): (60o,30o)

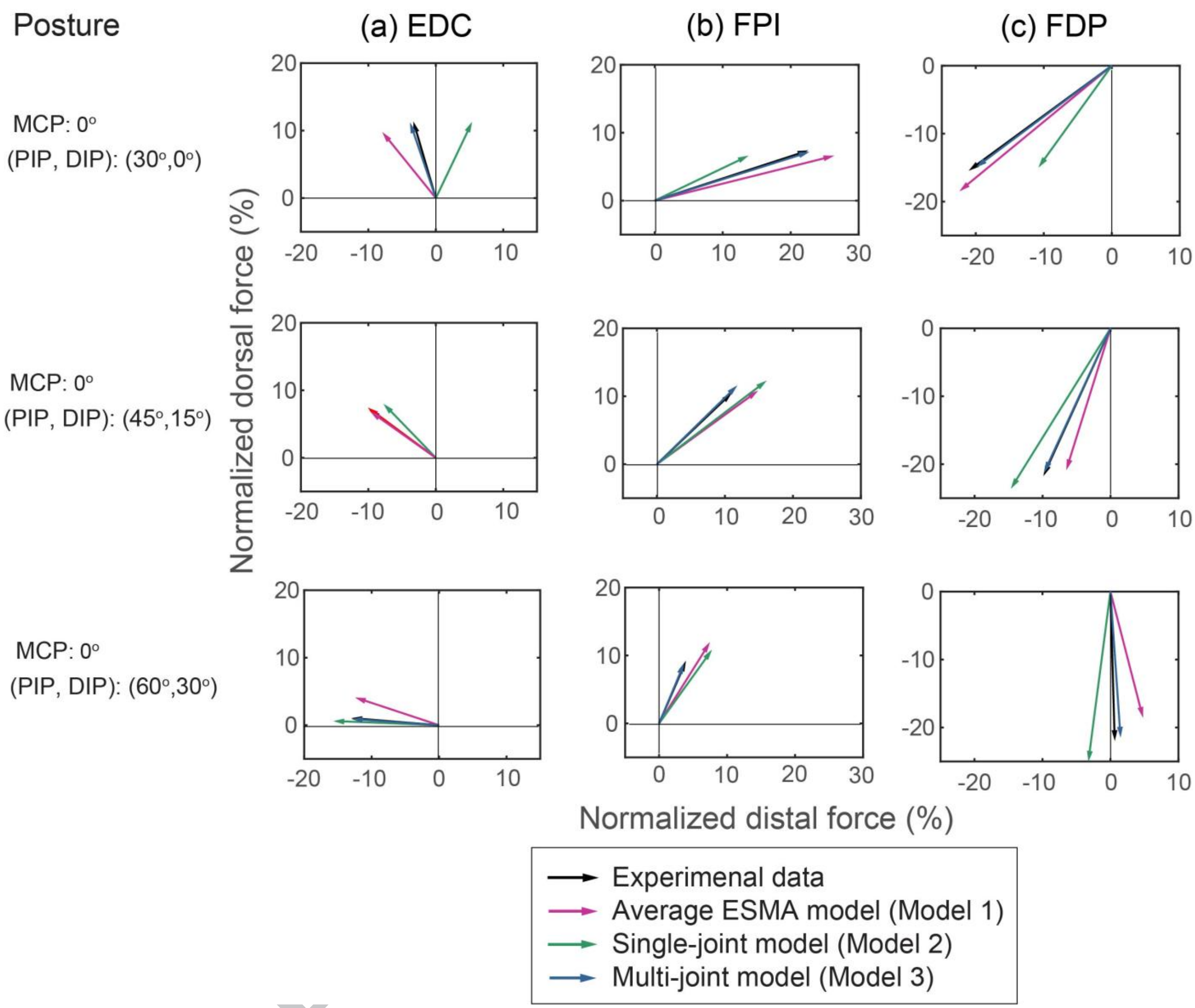

Posture
(a) EDC
(b) FPI
(c) FDP
MCP: 0°
(PIP, DIP): (30°,0°)
MCP: 0°
(PIP, DIP): (45°,15°)
MCP: 0°
(PIP, DIP): (60°,30°)
Normalized dorsal force (%)
Normalized distal force (%)
Experimenal data
Average ESMA model (Model 1)
Single-joint model (Model 2)
Multi-joint model (Model 3)